Int J Adv Manuf Technol (2013) 67:1161–1170
DOI 10.1007/s00170-012-4556-7

ORIGINAL ARTICLE

Occurrence of surface defects on strips during hot rolling process by FEM

Hai-liang Yu · Kiet Tieu · Cheng Lu · Guan-yu Deng · Xiang-hua Liu

Received: 13 July 2012 / Accepted: 3 October 2012 / Published online: 16 October 2012

Abstract During a hot rolling process, surface defects on strips can severely affect the quality of the rolled product, particularly for two conditions: (1) there are initial defects on continuous casting slabs that propagate and/or are inherited from those on the surface of rolled steels from upstream rolling processes; and (2) there are no initial defects on continuous casting slabs, and they consequently appear on the surface of rolled steels due to improper rolling technologies. In this paper, the authors present a new 3D finite element model coupled with constrained node failure to understand better the initiation and growth of surface defects on strips during the hot rolling process for case 2. The strip deformation processes were simulated for various rolling reduction ratios and friction coefficients between the roll and the strip. The occurrence of surface defects on strips was modeled under some rolling conditions. The plastic strain distribution in strips and the rolling forces were obtained. The risk of occurrence of surface defects on strips increases as the friction between the roll and strip increases for the same reduction ratio.

H.-l. Yu · K. Tieu · C. Lu · G.-y. Deng
School of Mechanical, Materials and Mechatronic Engineering,
University of Wollongong,
Wollongong, NSW 2500, Australia

H.-l. Yu (✉)
School of Mechanical Engineering, Shenyang University,
Shenyang 110044, China
e-mail: yuhailiang1980@tom.com

H.-l. Yu
e-mail: hailiang@uow.edu.au

X.-h. Liu
State Key Laboratory of Rolling and Automation,
Northeastern University,
Shenyang 110004, China

Keywords Surface defect · Hot rolling · Finite element method · Constrained node failure · Strip

1 Introduction

Surface defects of hot rolled steels are potentially serious problems during the rolling process because they might cause mill stoppage and rejection of the rolled materials. With more stringent requirement from customers and worker competition, surface defects have been paid more and more attention. However, there are many influencing factors that might result in surface defects on rolled steels in the following processes [1, 2]. The surface defects might occur for different reasons, but they can be divided into two categories: (1) there are initial defects on continuous casting slabs which propagate and/or are inherited from defects generated by upstream rolling processes [3] and (2) they are caused by improper rolling technologies and/or foreign bodies were rolled in the strip–roll interface. For case 1, we have many methods to avoid, such as cutting the slab edge and cleaning the slab surface, as shown in Fig. 1. And, some defects might be eliminated through a rolling process. However, for case 2, it will be difficult to avoid. Surface defects have often been found on multiphase steels [4, 5] and high silicon steels [6] whose slabs are of good surface quality before the rolling process.

The finite element method (FEM) has been widely used to analyze evolution of defects in strips during the rolling process [7]. Awais [8] and Son et al. [9] employed the 2D FEM and processing map to analyze the closure and growth of surface cracks on bars in the rolling process. Ervasti et al. [10, 11] simulated the closure and growth of longitudinal and transversal cracks in flat rolling process under a variety of crack sizes, roll radii, and friction coefficients. The authors [12, 13] have also simulated the behavior of transversal and longitudinal cracks on the slab surface during the vertical–horizontal

(a) Cutting slab edge (b) Cleaning slab surface

Fig. 1 Methods for preventing defect propagation. (**a**) Cutting slab edge, (**b**) cleaning slab surface

rolling process, and the contact pressure on the cracked surfaces was used to analyze the evolution of cracks. Deng et al. [14] simulated the closure behavior of inside cracks during a heavy plate rolling process by FEM, and they found that the minimum pass reduction needed for rectangular crack closing was about 13.9 %. Tang et al. [15] used the FEM to simulate the crack propagation in oxide scale under hot rolling conditions for different profile parameters of the oxide scale layer. Simulation results indicated that the larger was the initial profile surface roughness, the larger the crack width remaining after rolling. Yukawa et al. [16, 17] analyzed the deformation of the micro-cracks and the foreign bodies pressing in the rolling process by a 2D rigid-plastic FE code. In this case, the researches on the evolution of surface cracks by 2D thermo-mechanical FEM were carried out. Ghosh et al. [18] predicted the occurrence of edge cracks of aluminum alloys during cold rolling by taking the effective stress, equivalent plastic strain, and void volume fraction as a damage parameter. Xie et al. [19, 20] studied the edge crack propagation during cold rolling of a thin strip using FEM, and the optimum condition to eliminate defects was discussed. They also analyzed the influence of friction conditions on the evolution of edge cracks.

In the above literatures, the researchers generally assumed that the defects appeared on the strips before rolling and the meshing around defects were refined, and then investigated their evolution behavior during the rolling process. These works mainly have provided recommendations regarding removal of surface defects in continuous casting slabs (case 1 above) by analyzing which conditions the small defects will not propagate and/or eliminate. The authors [21] discussed three kinds of mechanisms for elimination of surface cracks during the rolling process. However, it is important to know what conditions the surface defects might appear on strips caused by rolling processes, so we can adjust the rolling technologies to avoid them, which will be valuable for dealing with the surface defects for case 2. 3D FE simulations have been carried out to understand better the crack initiation and growth at the edge of a silicon steel sheet during cold rolling process by Na and Lee [6], which is attributed to elastic deformation of work roll. The strain-controlled failure model was coupled with finite element method, and a series of FE simulations were carried out while three different roll bending modes were considered. In their models, the elements in the regions where the edge defects might appear should be refined to a certain small size because the failure elements were deleted. The typical failure behavior is caused by increasing the load with a non-uniform strain distribution. If the critical strain is exceeded, the structures will fracture. The strain failure model is widely used in plate, sheet material failure [6, 22–24]. The critical strains for different steel strip specimens could be obtained by uniaxial loading, etc.

In this paper, the authors present a new type of finite element model using constrained node failure method to simulate the occurrence of surface defects on strips during rolling. Finally, we focus on the influence of friction between the roll and strip on the surface quality of rolled steel for various reduction ratios. The calculated rolling forces by the method were in good agreement with that obtained by traditional FEM.

2 Theories and FE model

2.1 Surface defects on rolled strips

There are many surface defects that might appear on rolled strips, such as map/star/pattern cracks, transversal/longitudinal cracks, edge cracks, edge black defects, and scale

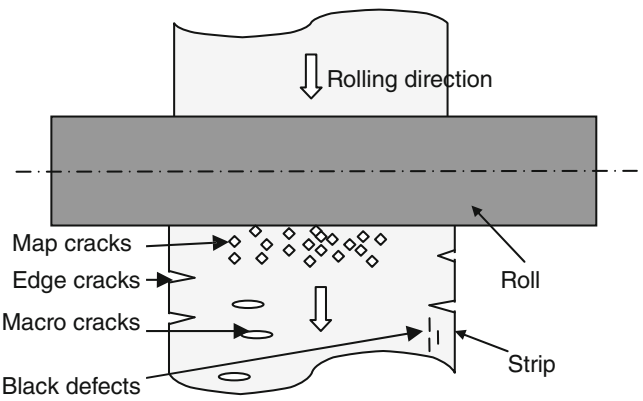

Fig. 2 Surface defects in strips after the rolling process

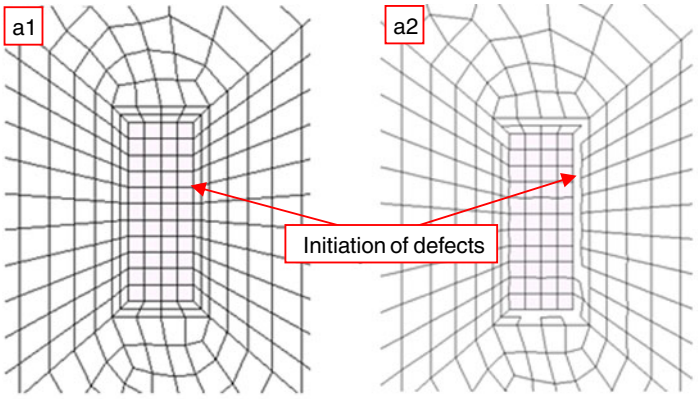

(a) Method by element kill(Before deformation (a1); after deformation(a2))

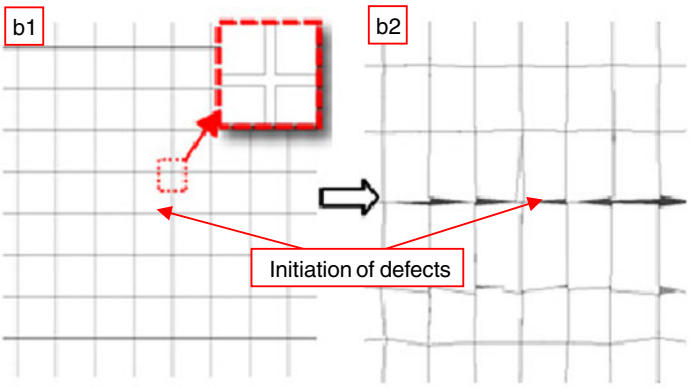

(b) Method by elements constrains failure(before deformation (b1); after deformation(b2))

Fig. 3 Illustration of occurrence of defects by using FEM. **a** Method by element kill (before deformation, *a1*; after deformation, *a2*). **b** Method by element constrain failure (before deformation, *b1*; after deformation, *b2*)

marks. Figure 2 shows the illustration of four typical surface defects on a strip during rolling process. The map cracks often appear on the full surface of the strip, which might be caused by the structure stress on the strip surface in the flame scarfing process and/or overheating in local regions by a non-uniform heating in the reheat furnace. The edge cracks might appear during the rolling process because the stress strength at the strip edge is greater than the maximum tensile stress of the materials. The macro cracks contain transversal and longitudinal cracks. Their origin is similar to that of edge cracks which might result in strip breakage during rolling. The black defects present themselves as continuous small defects near the edge, which might be caused by the non-uniform temperature near the strip edge during the rolling process and/or the movement of the strip edge side surface to the strip up/down surfaces during roughing. The above four kinds of surface defects on strips might occur in the rolling processes where there are no initial defects on the continuous casting slabs. They might all be caused by the non-uniform deformation in local regions during a rolling process that results in the excessive stress concentration in local regions well above the maximum tensile strength of the materials. Thus, the FE models presented here to simulate the occurrence of the above surface defects during a rolling process should not contain any initial defects.

Owing to the spread behavior of strips during hot rolling, the strain and stress distributions are non-uniform along strip width and rolling directions. The defects will appear at the location where the strain is larger than the critical value. Na and Lee [6] employed the FE models by element

Table 1 Coefficient of parameters in Eq. (1)

Coefficient	*A*	*B*	*C*	*D*	*F*
Value	1,715.706	0.17311	0.16952	0.05515	−0.267881

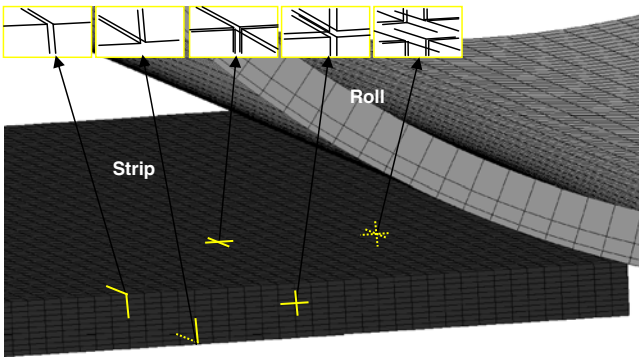

Fig. 4 Geometrical and FE meshing of the strip rolling process

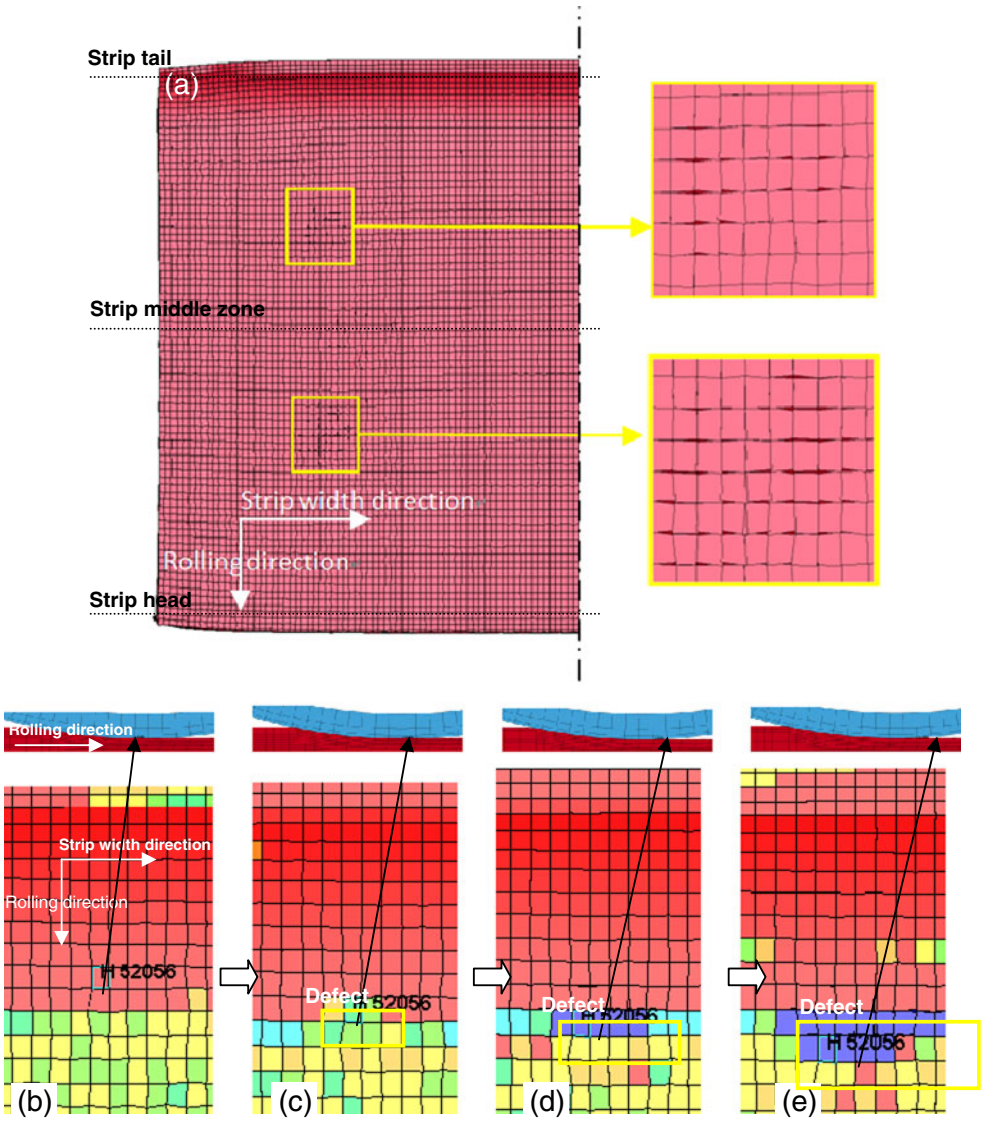

Fig. 5 Surface defects occur on the strip after rolling with reduction ratio, 45 %; critical failure strain, 1.4; and friction coefficient, 0.35

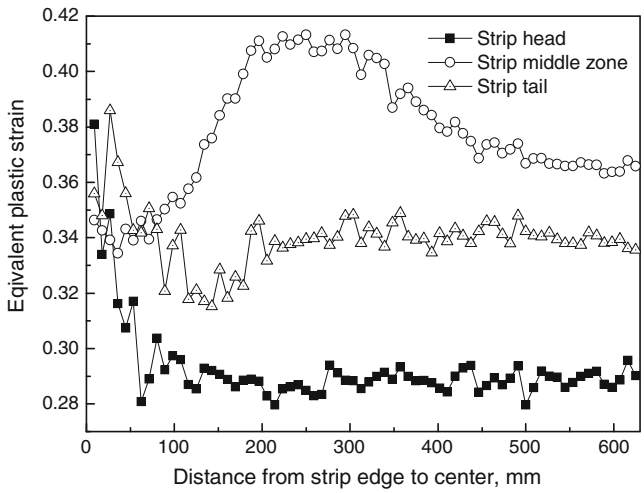

Fig. 6 Equivalent plastic strain along strip width direction when the reduction ratio is 25 %

kill method to simulate the occurrence of edge cracks during the cold rolling process. An illustration of the element kill method is shown in Fig. 3a. When the plastic strain of an element reaches the critical failure value, the element will be killed and not calculated in the following steps. The method requires refining the elements to a certain small size, which is suitable to simulate certain defects, such as edge defects where the elements near the strip edge could be refined. If it is employed to predict the occurrence of defects at an unknown position, it will require a prohibitive huge number of elements. Figure 3b shows the method by constrained node failure for simulating the occurrence of defects. In the models, every element is established by their eight nodes, and there is a very small space between the adjacent elements; the adjacent nodes are constrained with critical failure strain, and the defects will occur if the calculated value is larger than it. Compared with the method by element kill, the method by constrained node failure does not need a large

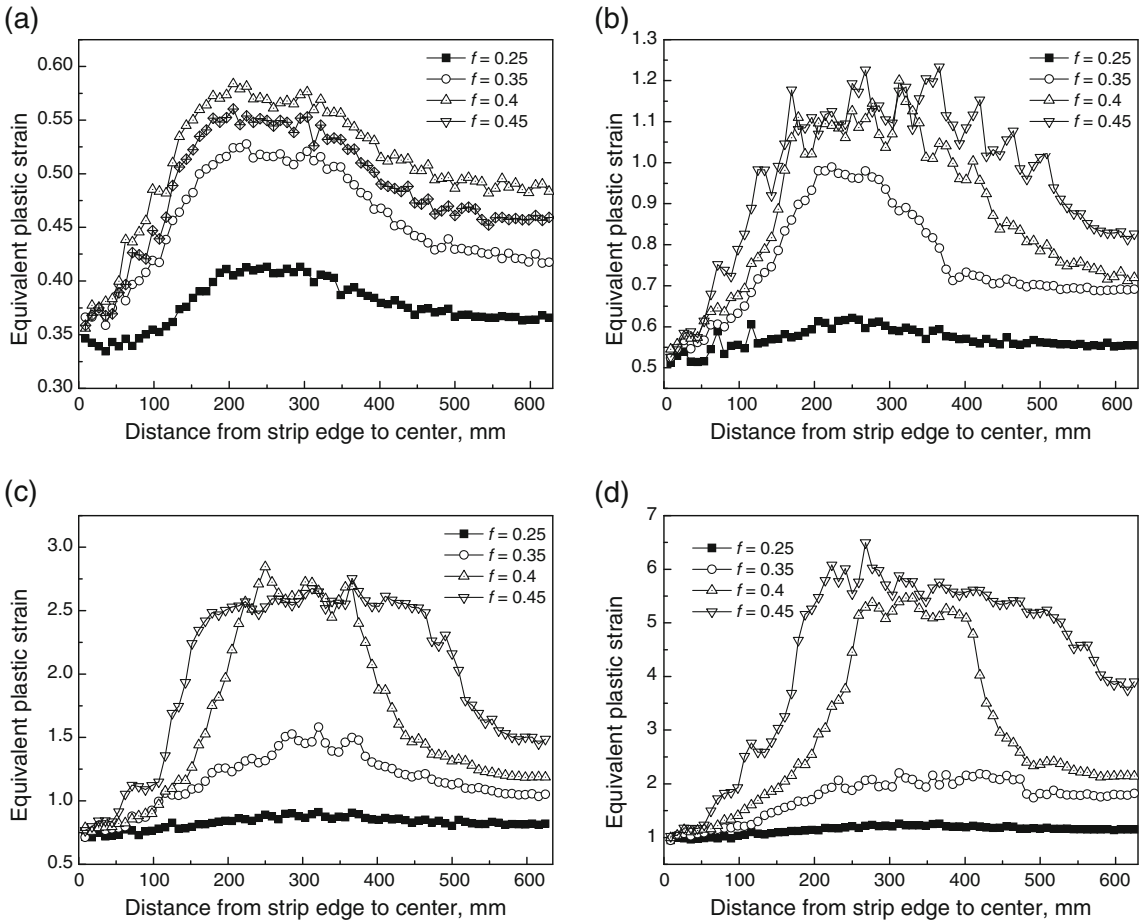

Fig. 7 Equivalent plastic strain along the strip width direction under various friction coefficients for the reduction ratios 25 % (**a**), 35 % (**b**), 45 % (**c**), and 55 % (**d**)

number of elements although it needs to define a series of constrain for every group of adjacent nodes.

2.2 Parameters and models

In this paper, the method by constrained node failure is employed to simulate the occurrence of surface defects on strips during the rolling process. The roll diameter is 825 mm, and the strip profile sizes before rolling are 1,250 mm width × 40 mm thickness [25]. The roll is considered as rigid. The isotropic plasticity material model is employed for the strips. Four reduction ratios, 25, 35, 45, and 55 %, were analyzed. In the simulation, the critical plastic strain at failure is employed to judge failure. During this simulation, the yield stresses of strips were computed by Eq. (1).

$$\sigma_0 = A\varepsilon^B \dot{\varepsilon}^{CT+D} e^{FT} \tag{1}$$

where ε is true strain; $\dot{\varepsilon}$ is true strain rate; T is the deformation temperature which is assumed to be 1,100 °C; and A, B, C, D, and F are material constants as listed in Table 1.

Taking consideration of symmetry, a quarter of rolling model was employed in the FE models. The strip was established by eight-noded hexahedral elements which were independent of each other. The adjacent nodes were constrained. The roll was meshed by eight-noded hexahedral elements by traditional meshing method. There were 518,800 nodes and 108,392 elements in the strip and roll. The geometry model and FE meshing of the rolling process is shown in Fig. 4. There are three types of relationships between adjacent nodes. (1) The nodes in the edges of the strip (12 lines), two adjacent nodes, are set up as groups considering plastic strain failure. (2) The nodes in the outer surface of the strip (six surfaces), four adjacent nodes, are set up as groups considering plastic strain failure. (3) The nodes in the inner body of the strip, eight adjacent nodes, are set up as groups considering plastic strain failure. During the rolling process, the strip enters the roll gap with an initial velocity of 0.8 m/s, and the velocity of the roll surface is 0.85 m/s. The Coulomb friction model was employed to decide the friction behavior between the strip and the roll. Four friction coefficients (f, in the figures as follows), 0.25, 0.35, 0.4, and 0.45, were used.

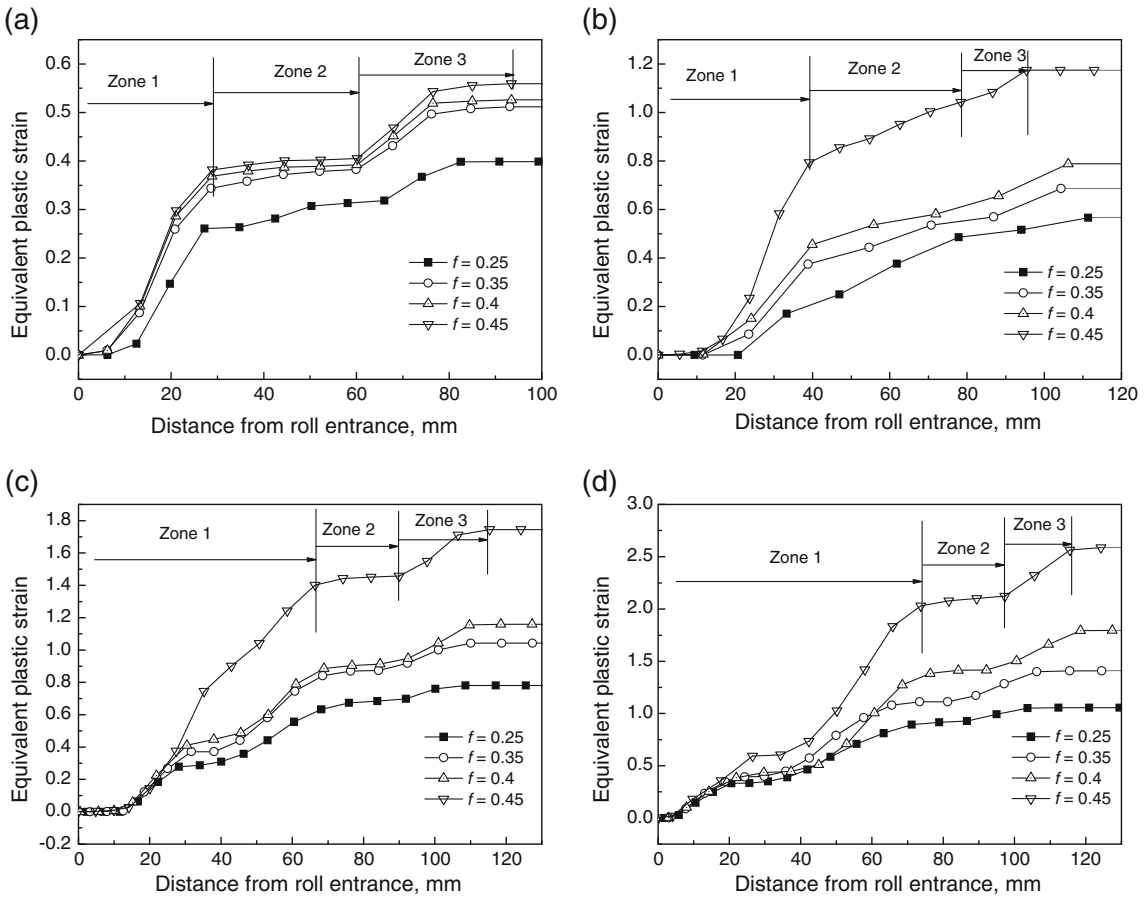

Fig. 8 Change of the strain of element at one-fourth strip width in the strip middle zone in the rolling deformation zone for the reduction ratio 25 % (**a**), 35 % (**b**), 45 % (**c**), and 55 % (**d**)

3 Results and discussion

Figure 5 shows that surface defects occur on a strip after rolling when the reduction ratio is 45 %, critical failure strain 1.4, and friction coefficient 0.35. Figure 5 (a) shows the whole strip after the rolling process. Under the rolling conditions, the surface defects mainly occur at one-eighth width from the strip edge. Figure 5 (b–e) shows the occurrence and evolution of a defect in the rolling deformation zone. In Fig. 5 (b), the element H52056 passes through the forward zone without defects. With further rolling deformation, the element H52056 and its two neighbor elements fail first, and a small defect firstly appears, and then it gradually propagates. Meanwhile, the concentration stress in this zone disappears with the

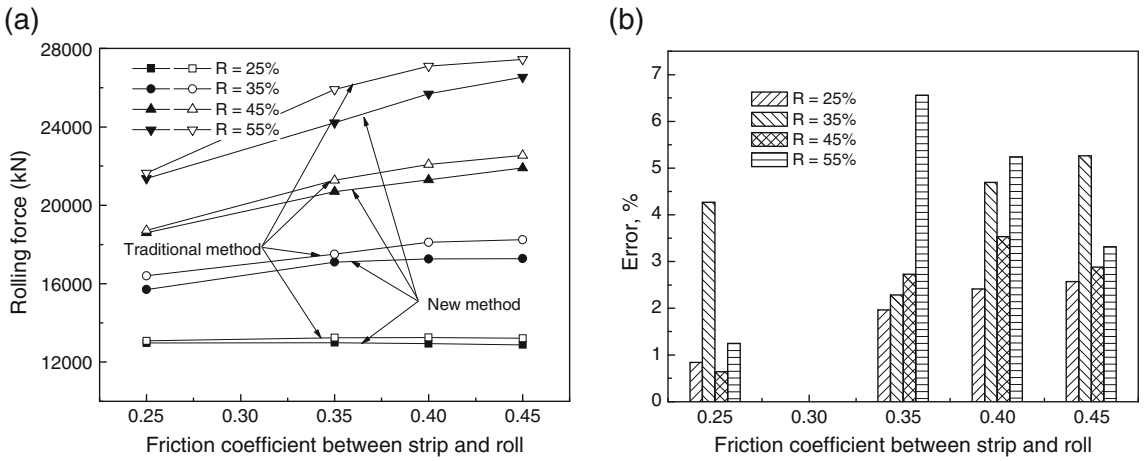

Fig. 9 Rolling forces under different rolling conditions

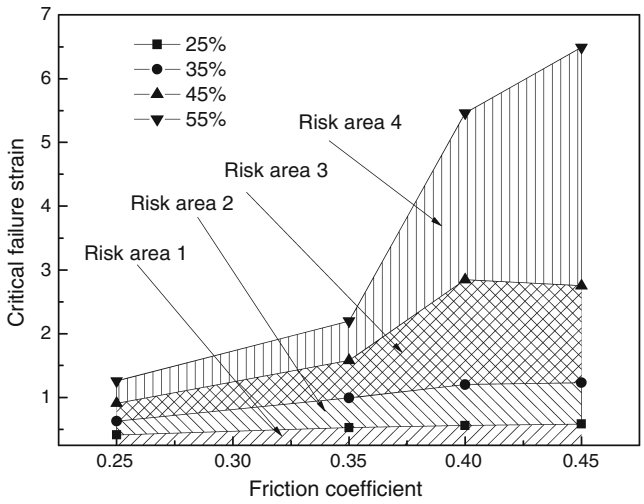

Fig. 10 Risk for occurrence of surface defects for plastic failure during the rolling process

occurrence of defects, as shown in Fig. 5 (c–e) (The color in figures shows the stress distribution in the strip).

Figure 6 shows the equivalent plastic strain distribution along the strip width direction when the reduction ratio is 25 % and the friction coefficient is 0.25, where the positions of strip head, middle zone, and tail are shown in Fig. 5. In the figure, the equivalent plastic strain at the strip middle zone is greater than that at the strip head and tail with the same position along strip width direction, which is caused by the freedom constraining in the strip middle zone for front and rear regions in the rolling deformation zone. Thus, only the equivalent plastic strain at the strip middle zone is analyzed because the failure parameter is the plastic strain between constrained nodes in the models, and thus, the defects will firstly occur at the larger plastic strain zones.

Figure 7 shows the equivalent plastic strain distribution at the strip middle zone under a variety of friction coefficients and reduction ratios for the reduction ratio (a) 25 %, (b) 35 %, (c) 45 %, and (d) 55 %. In the figures, the equivalent plastic strain increases with increase of the friction coefficient except the strip edge zone. As reduction ratios increase, the maximum equivalent plastic strain gradually moves to the strip central zones. For that, the surface defects will affect the whole surface quality of the strip at higher reduction.

Figure 8 shows the change of the equivalent plastic strain of the element at one-fourth strip width in the strip middle zone in the rolling deformation zone under various reduction ratios, for reduction ratio (a) 25 %, (b) 35 %, (c) 45 %, and (d) 55 %. In the figures, the change of equivalent plastic strain could be divided into three stages corresponding with the forward slip zone (zone 1), stick zone (zone 2), and backward slip zone (zone 3). When the reduction ratio is 25 %, the three stages of equivalent plastic strain in the rolling deformation zone under various friction coefficients change slightly, as shown in Fig. 8a. With an increase in the reduction ratios, the differences among them gradually increase. And, it can be seen clearly that the strain in "zone 1" increases while those in "zone 2" and "zone 3" do not increase so much. Meanwhile, the influence of friction on the change of equivalent plastic strain increases with increasing reduction ratios. When the reduction is certain, the period of "zone 1" increases as low friction, while the equivalent plastic strain increases greatly in the period, as shown in Fig. 8c and d.

Figure 9 shows the rolling force under different rolling conditions by the proposed method and the traditional FEM.

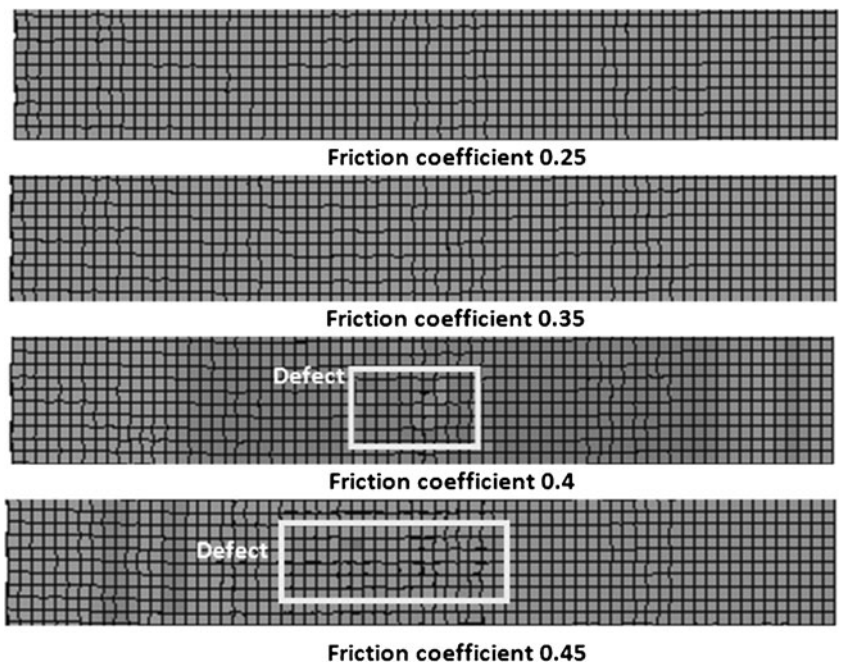

Fig. 11 Surface defects on strips after rolling process under various frictions for failure strain 1.1

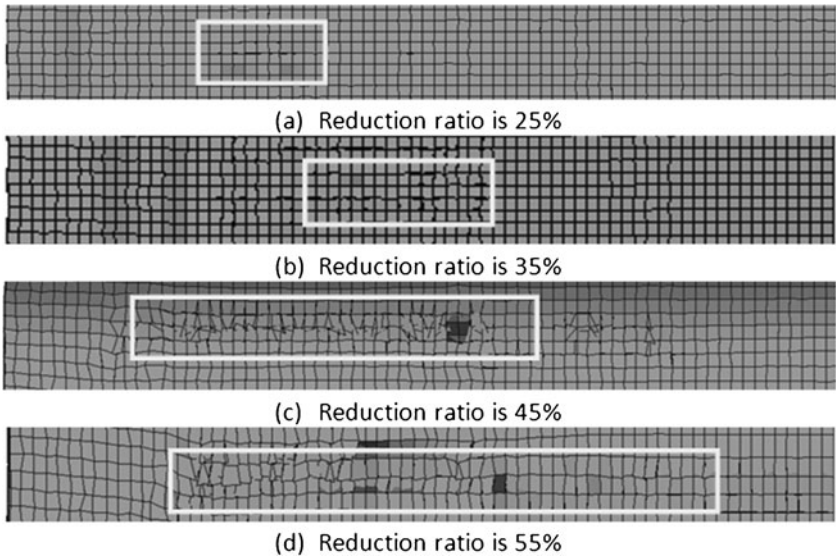

Fig. 12 Surface defects on strips after rolling process for various reduction ratios with the friction coefficient 0.45

In the models, the rolling force by using the new method marches well with that by the traditional FEM although the former is a little lower. In the models with the new method, there are small spaces between elements where there is no contact force, which results in reduction of the rolling force. Figure 9b shows the error between two methods, which is acceptable in the rolling production. Through analysis of the rolling force, the FE model coupled constrained node failure could be used to simulate the strip deformation during the rolling process.

From the results above, we could find that the equivalent plastic strain increases with increase in friction. For the hard deformation steels, the materials might fail when their plastic strains are greater than critical value. When the critical failure strain is less than the equivalent plastic strain, the defects will occur at the strips. According to the equivalent plastic strain in the strip during the rolling process, we could get the critical failure strain. Figure 10 shows the risk for occurrence of surface defects on strips during the rolling process, where the risk areas 1~4 are for the reduction ratio 25~55 % separately. When the reduction ratio is 25 % and the critical plastic strain failure of materials fills in "risk area 1," the surface defects on the strips will occur. When the reduction ratio is 35 % and the critical plastic strain failure of materials fills in "risk area 2" and "risk area 1," the surface defects on the strip will appear. When the reduction ratio is 55 %, the risk for appearance of surface defects will greatly increase when the friction coefficient is 0.4~0.45. In the figure, the risk for occurrence of surface defects on strips increases as the friction between the roll and strip increases. Figure 11 shows the occurrence of surface defects on the strip under various frictions when the reduction ratio is 35 %. In Tang's work [15], they also pointed out that the crack width retained on the strip surface is larger the higher the roll surface roughness.

The surface defects approach the strip edge with an increase in the friction coefficients when the reduction ratio is about 25 %; for that, the black defects or simple macro

Fig. 13 Surface defects in a strip after hot rolling

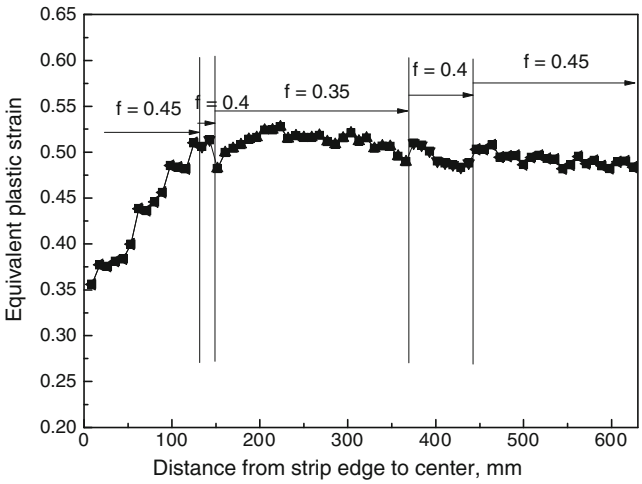

Fig. 14 Equivalent plastic strain distribution using subregion lubrication

defects will occur first. When the reduction ratio is about 45 % and the friction coefficient is 0.45, the high plastic strain occurs about three fourths of the strip width; under these rolling conditions, the map cracks might appear. In Fig. 7, with increasing reduction, the range of equivalent plastic strain as high value increases greatly when the friction coefficient is 0.45. Figure 12 shows the surface defects on strips under some rolling conditions when the friction coefficient is 0.45. For that, the risk for occurrence of map defects will increase. Results in Fig. 12, d, agree qualitatively with test results in Fig. 13. Meanwhile, in the models, it could be found that the equivalent plastic strain at the strip edge changes slightly for a variety of friction coefficients. Under these conditions, the non-uniform deformation behavior at the strip edge will increase with both reduction ratio and friction coefficient. The non-uniform strain increases until it reaches the critical strain when cracks occur.

During the rolling process, it is expected that the deformation of strips is uniform for decreasing the surface defects. When the friction between the strip and roll was large, lubrication could be employed in the rolling process. In Fig. 7, the equivalent plastic strain from the strip edge to the center first increases greatly and then increases slowly, keeps on a range of maximum value, and then reduces greatly and keeps uniformly until strip center. According to the regularity, Fig. 14 shows the equivalent plastic strain distribution when the rolling zone was divided as five subregions along the strip width direction obtained from Fig. 7a. Under this condition, the risk for appearance of surface defects will decrease.

4 Conclusions

1. A finite element model coupled with the constrained node failure method has been successfully developed to simulate the occurrence of surface defects on strips during the hot rolling process. The FEM model can predict that the defects will occur if the parameter of failure criterion is larger than the criteria value.
2. As friction between the strip and roll increases, it may promote the occurrence of surface defects on the strips. As reduction ratios increase, the defects gradually move to the strip central zone.
3. The calculated rolling forces by the new method were in good agreement with that by the traditional finite element method.

Acknowledgments The authors gratefully acknowledge the financial support from the National Natural Science Foundation of China through 51105071, the Doctorate Foundation of the Ministry of Education of China through grant. 20090042120005, and the Vice-Chancellor's Fellowship Grant at the University of Wollongong.

References

1. Tercelj M, Turk R, Kugler G, Perus L (2008) Neural network analysis of the influence of chemical composition on surface cracking during hot rolling of AISID2 tool steel. Comput Mater Sci 42:625–637
2. Pandey JC, Raj M, Choubey PN (2009) Split ends and cracking problem during hot rolling of continuously cast steel billets. J Fail Anal Preven 9:88–96
3. Che YM, Zhu T, Zhang HM, Dong M, Chen QA (2006) Surface defects of CSP strip, sheets from cold rolled and galvanized strip. Iron Steel 41:63–66
4. Uthaisangsuk V, Prahl U, Bleck W (2011) Modelling of damage and failure in multiphase high strength DP and TRIP steels. Eng Fract Mech 78:469–486
5. Murakami T, Kinefuchi M, Nomura M, Mukai Y (2008) Effects of hot rolling conditions on the fatigue limit of Ti added dual phase hot-rolled steel sheets. J Jpn Inst Metals 72:832–838
6. Na DH, Lee Y (2008) FE simulation of edge crack initiation and propagation of conventional grain orientation electrical steel. Int J Mod Phys B 22:5465–5470
7. Liu X (2010) Progress and application of plastic finite element method in metals rolling process. Acta Metall Sin 46: 1025–1031
8. Awais M, Lee HW, Im YT, Kwon HC, Byon SM, Park HD (2008) Plastic work approach for surface defect prediction in the hot bar rolling process. J Mater Process Technol 201:73–78
9. Son IH, Lee HD, Choi S, Lee DL, Im YT (2008) Deformation behavior of the surface defects of low carbon steel in wire rod rolling. J Mater Process Technol 201:91–96
10. Ervasti E, Ståhlberg U (1999) Behavior of longitudinal surface cracks in the hot rolling of steel slabs. J Mater Process Technol 94:141–150
11. Ervasti E, Ståhlberg U (2000) Transversal cracks and their behavior in hot rolling of steel slabs. J Mater Process Technol 101:312–321
12. Yu HL, Liu XH, Li CS, Lan FF, Wang GD (2009) Research on the behavior of transversal crack in slab V-H rolling process by FEM. J Mater Process Technol 209:2876–2886
13. Yu HL, Liu XH, Ren XJ (2008) Behavior of longitudinal cracks in slab V-H rolling processes. Steel Res Int 79:537–543
14. Deng W, Zhao DW, Qin XM, Du LX, Gao XH, Wang GD (2009) Simulation of central crack closing behavior during ultra-heavy plate rolling. Comput Mater Sci 47:439–447
15. Tang J, Tieu AK, Jiang Z (2006) Modelling of the development of initial crack under hot rolling condition. Mater Sci Forum 505–507:1291–1296
16. Yukawa N, Ishikawa T, Yoshida Y, Koyachi A (2005) Influence of rolling condition on deformation of surface micro-defect in plate rolling. Tetsu-to-Hagané 91:861–867
17. Yukawa N, Yoshida Y, Ishikawa T (2006) Deformation analysis of longitudinal surface micro-defects in flat rolling. Tetsu-to-Hagané 92:19–24
18. Ghosh S, Li M, Gardiner D (2004) A computational and experimental study of cold rolling of aluminum alloys with edge cracking. J Manuf Sci Eng 126:74–82
19. Xie HB, Jiang ZY, Wei DB, Tieu AK (2010) Study on edge crack propagation during cold rolling of thin strip by FEM. AIP Conf Proc 1252:1320–1325
20. Xie HB, Jiang ZY, Yuen WYD (2011) Analysis of friction and surface roughness effects on edge crack evolution of thin strip during cold rolling. Tribol Int 44(9):971–979

21. Yu HL, Liu XH (2009) Thermal-mechanical FE analysis of evolution behavior of slab surface cracks during hot rolling. Mater Manuf Process 24(5):570–578
22. Jeschke J, Ostermann D, Krieg R (2011) Critical strains and necking phenomena for different steel sheet specimens under uniaxial loading. Nucl Eng Des 241:2045–2052
23. Elangovan K, Narayanan CS, Narayanasamy R (2011) Modelling the correlation between the geometrical features and the forming limit strains of perforated Al 8011 sheets using artificial neural network. Int J Mater Eng Appl 4:389–399
24. Verleysen P, Peirs J, Van Slycken J, Faes K, Duchene L (2011) Effect of strain rate on the forming behaviour of sheet metals. J Mater Process Technol 211:1457–1464
25. Yu HL, Liu XH, Chen LQ, Li CS, Zhi Y, Li XW (2009) Influence of edge rolling reduction on plate-edge stress during finish rolling process. J Iron Steel Res Int 16:22–26